The Astrophysical Journal Supplement Series, 173:512–523, 2007 December

THE EFFECT OF ENVIRONMENT ON THE ULTRAVIOLET COLOR-MAGNITUDE RELATION OF EARLY-TYPE GALAXIES

K. Schawinski,[1] S. Kaviraj,[1] S. Khochfar,[1] S.-J. Yoon,[2,1] S. K. Yi,[2,1,] J.-M. Deharveng,[3] A. Boselli,[3] T. Barlow,[4] T. Conrow,[4] K. Forster,[4] P. G. Friedman,[4] D. C. Martin,[4] P. Morrissey,[4] S. Neff,[5] D. Schiminovich,[6] M. Seibert,[4] T. Small,[4] T. Wyder,[4] L. Bianchi,[7] J. Donas,[3] T. Heckman,[7] Y.-W. Lee,[2] B. Madore,[8] B. Milliard,[3] R. M. Rich,[9] and A. Szalay[7]

Received 2005 November 2; accepted 2005 December 28

ABSTRACT

We use *GALEX* near-UV (NUV) photometry of a sample of early-type galaxies selected in the SDSS (Sloan Digital Sky Survey) to study the UV color-magnitude relation (CMR). NUV $-$ r color is an excellent tracer of even small amounts ($\sim$1% mass fraction) of recent ($\lesssim$1 Gyr) star formation, and so the NUV $-$ r CMR allows us to study the effect of environment on the recent star formation history. We analyze a volume-limited sample of 839 visually inspected early-type galaxies in the redshift range $0.05 < z < 0.10$ brighter than M_r of -21.5 with any possible emission-line or radio-selected active galactic nuclei (AGNs) removed to avoid contamination. We find that contamination by AGN candidates and late-type interlopers highly bias any study of recent star formation in early-type galaxies and that, after removing those, our lower limit to the fraction of massive early-type galaxies showing signs of recent star formation is roughly 30% $\pm$ 3%. This suggests that residual star formation is common even among the present day early-type galaxy population. We find that the fraction of UV-bright early-type galaxies is 25% higher in low-density environments. However, the density effect is clear only in the lowest density bin. The blue galaxy fraction for the subsample of the brightest early-type galaxies, however, shows a very strong density dependence, in the sense that the blue galaxy fraction is lower in a higher density region.

Subject headings: galaxies: elliptical and lenticular, cD — galaxies: evolution — galaxies: formation — galaxies: fundamental parameters

1. INTRODUCTION

There is observational evidence pointing to a very simple evolutionary model for early-type galaxies. This model of *monolithic collapse* was first proposed by Eggen et al. (1962) to explain the origin of the Milky Way halo. According to this model, the Milky Way halo formed through the rapid collapse of a cloud of gas very early on in the history of the universe, forming all of its stars in an initial burst followed by a passive evolution of the stellar population. A similar model is often invoked as the simplest explanation for the old and seemingly homogeneous stellar populations seen in early-type galaxies (Larson 1975).

The apparently universal relationship between galaxy color and luminosity in early-type galaxies was first studied in detail by (Visvanathan & Sandage 1977) even though the relation had been observed before (Baum 1959; de Vaucouleurs 1961; McClure & van den Bergh 1968). This *color-magnitude relation* (CMR) is often used as a tool for understanding the formation and evolution of early-type galaxies.

A seminal investigation on the optical CMR was undertaken by Bower et al. (1992) on the elliptical galaxies in the Virgo and Coma clusters. Their study revealed a remarkably small intrinsic scatter around the mean relation. In the context of the monolithic paradigm, they interpreted the small scatter as the result of a small age dispersion among galaxies of the same age and the slope as a result of a mass-metallicity relation (Kodama & Arimoto 1997). Furthermore, they concluded that massive early-type galaxies did not have any major episodes of star formation at redshifts $z < 2$.

More massive galaxies are likely to be in deeper potential wells and are therefore more able to retain metals ejected from supernovae from the initial generations of young stars at high redshift, leading to the observed mass-metallicity relation (Larson 1974). In addition to this, the observed levels of α-enhancement (Worthey et al. 1992; Carollo et al. 1993; Carollo & Danziger 1994a, 1994b; Kodama & Arimoto 1997; Trager et al. 2000) in many giant ellipticals imply that the initial formation starburst was of a very short duration, less than 1 Gyr (Bruzual & Charlot 1993; Thomas et al. 1999).

Later studies have found that there is no significant evolution in the optical CMR out to $z = 1$ and further (Ellis et al. 1997; Gladders et al. 1998; Stanford et al. 1998; van Dokkum et al. 2000; Blakeslee et al. 2003; Ferreras et al. 2005). All this adds up to a picture of massive early-type galaxies forming in an initial, intense starburst at high redshift followed by a relatively passive evolution.

However, we know since the simulations of (Toomre & Toomre 1972) that the product of a spiral-spiral merger can be an elliptical galaxy (Negroponte & White 1983; Barnes 1988; Hernquist 1992; Naab & Burkert 2003). An alternative approach to understanding early-type galaxies takes into account dynamical interactions and mergers. In the *Hierarchical Merger* paradigm, small galaxies form first and later assemble into larger objects (White & Rees 1978).

The advent of semianalytical models (SAMs) in the 1990s has greatly enhanced our understanding of galaxy evolution in such

[1] Department of Physics, University of Oxford, Oxford OX1 3RH, UK.
[2] Center for Space Astrophysics, Yonsei University, Seoul 120-749, Korea.
[3] Laboratoire d'Astrophysique de Marseille, 13376 Marseille Cedex 12, France.
[4] California Institute of Technology, MC 405-47, Pasadena, CA 91125.
[5] Laboratory for Astronomy and Solar Physics, NASA Goddard Space Flight Center, Greenbelt, MD 20771.
[6] Department of Astronomy, Columbia University, MC 5246, New York, NY 10027.
[7] Department of Physics and Astronomy, Johns Hopkins University, Baltimore, MD 21218.
[8] IPAC,770 South Wilson Avenue, Pasadena, CA 91125.
[9] Department of Physics and Astronomy, University of California, Los Angeles, CA 90095.

a hierarchical universe. Kauffmann et al. (1996) find that in the Canada-France Redshift Survey, only 1/3 of elliptical and lenticular galaxies at redshift $z = 1$ were fully assembled and showed colors expected of old passively evolving systems. There is of course older evidence for a strong dependence of the population of early-type galaxies on density and redshift. Dressler (1980) found that approximately 80% of galaxies in a sample of 55 clusters were of early-type morphology, a much higher fraction than in the field, suggesting that the denser cluster environment does affect galaxy evolution. When Butcher & Oemler (1984) looked at higher redshift clusters, they found that the fraction of blue, spiral galaxies in cluster environments increased with redshift. Later studies confirmed that this trend was not a selection effect (Dressler et al. 1997; van Dokkum et al. 2000). This evolution is accompanied with an increase in merger rates (Couch et al. 1998; van Dokkum et al. 1999; Khochfar & Burkert 2001).

In a purely monolithic collapse model, the star formation history of early-type galaxies is almost trivial, as they are composed of uniformly old stars. As soon as we allow for any sort of hierarchical merging, the story becomes much more complex. Rather than being uniform, the star formation histories become highly degenerate, as disparate stellar populations from progenitor galaxies are mixed together. Beyond this simple addition, the merging history of the galaxy and its progenitors adds further complication as entirely new populations are created during interactions and mergers. Thus, assigning a single age to the stellar population of an early-type galaxy is misleading—there is no single age. The typically derived luminosity-weighted ages are in this sense nontrivial to interpret. We know now that the combined effects of age, dust, metallicity, and—potentially—a multitude of progenitors are highly degenerate. Bower et al. (1992) took the apparent uniformity and low intrinsic scatter as a very strong constraint on the evolution of the Virgo & Coma early-type population. While monolithic evolution is the simplest possible explanation of these observations, however, it does not necessarily exclude other interpretations.

Kaviraj et al. (2005) have argued using merger models that the optical early-type CMR is useful for constraining evolution models *only* if we believe a priori in a monolithic model. The effect of progenitor bias—the fact that a progressively larger fraction of the progenitor set of present-day ellipticals is contained in late-type star-forming galaxies at higher redshift—means that we are *not* probing the entire star formation history of early-type galaxies, but rather a progressively more biased subset. Besides, the level of star formation predicted by SAMs incorporating AGNs and supernova feedback is very low; on the order of a few percent by stellar mass. Optical filters, including U band, are not sufficiently sensitive to detect such a low-level star-forming activity. This is why we must turn to the UV.

The *Galaxy Evolution Explorer* (*GALEX*; Martin et al. 2005) near-UV filter is capable of detecting even a small ($\sim$1% mass fraction) young stellar population and so ideal for tracing the recent star formation history of early-type galaxies. The UV color-magnitude relation allows us to identify the last important episode of star formation in galaxies. Yi et al. (2005) have already shown using *GALEX* information that a significant fraction of massive early-type galaxies at low redshift exhibit levels of star formation undetectable in the optical but visible in the UV. Our paper presents the results of our search for the effect of environment on the recent star formation.

We assume a standard ΛCDM cosmology with $(\Omega_M, \Omega_\Lambda) = (0.3, 0.7)$ and a Hubble constant of $H_0 = 70$ km s^{-1} Mpc^{-1} (Spergel et al. 2003).

2. SAMPLE SELECTION

The *GALEX* Medium Imaging Survey (MIS) is a wide-area survey with limiting magnitudes of 22.6 AB in the far-UV (FUV; 1344–1786 Å) and 23.0 AB in the near-UV filter (NUV; 1771–2831 Å) (Morrissey et al. 2005) with substantial overlap with the Sloan Digital Sky Survey DR3 (Stoughton et al. 2002; York et al. 2000; Abazajian et al. 2005). We define a sample of early-type galaxies within SDSS and then cross-match it to *GALEX* detections. We use the *GALEX* Internal Release 1.1 MIS data.

2.1. *Early-Type Galaxy Selection in SDSS*

A fundamental problem in the study of early-type galaxies is that there are no fixed criteria for their classification. In terms of the Hubble sequence, everything equal to or earlier than a lenticular is an early-type galaxy, but even this innocent definition is highly subjective, varies between different observers, and strongly depends on the image quality used to evaluate it. There is danger in classifying galaxies as early-types using the properties that are based on the presumption that early-type galaxies are old, red, dead, uniform, and dustless, e.g., colors or spectral features. By making such supposition, any subpopulation of early-type galaxies departing from this set of prejudices is liable to be rejected. Such a sample is then biased against *precisely those* early-type galaxies that can tell us the most about galaxy evolution.

In order to create an unbiased, volume-limited sample, we match *GALEX* NUV detections to a catalog of early-type galaxies identified in the SDSS. The paramount effort of Bernardi et al. (2003a, hereafter B03) has already generated such a catalog of $\sim$9000 galaxies. They were selected on a number of SDSS pipeline parameters. Such a catalog is no doubt extremely useful for studying the overall properties of galaxies in a statistical sense but less than perfect to our investigation, which is searching for "abnormality" of early-type galaxies. For instance, B03 uses the Principal Component Analysis Technique, which is biased strongly against star-forming ellipticals (e.g., Fukugita et al. 2004). Second, the sample generated this way is bound to be contaminated by late-type interlopers despite the effort of cleaning the sample in various ways (see B03 for details). In a visual inspection of a sample of bright ($M_r < -22$) early-types from the B03 catalog, we found up to 30% contamination. These were not only Sa galaxies with small or faint spiral arms, but also edge-on disk and a number of face-on spirals. Such late-types are generally actively star-forming and should be removed from our sample. Besides, it is difficult to estimate the rate of false rejections (that is, early-types falsely rejected) if we use a catalog generated by a different group a priori. Some of these false rejections may be due to the *spectral* part of the B03 criteria. Rich et al. (2005) find the same contamination problem when they employed a method similar to B03.

To avoid these problems, we define a simple set of *morphology-driven* criteria with no assumptions at all on color or spectral energy distribution (SED). We define early-type galaxies to be those bulge-dominated galaxies that lack clearly visible spiral arms. We use these criteria to create an *inclusive* rather than *exclusive* sample to avoid rejecting too many genuine early-types. In order to select early-type galaxies over late-types, we consider the surface-brightness profiles in three bands and select those which have a very high likelihood of being a de Vaucouleurs profile rather than an exponential profile. To do this, we use the `fracDev` parameter, which is the weight of the de Vaucouleurs profile of the linear combination that best fits the image in each band. We select galaxies in DR3 with the following parameters:

1. *SED quality.*—The spectrum is of good quality (S/N > 10).
2. `fracDev_g` > 0.95.—We use the *g* profile as it is sensitive to blue disk and arm stellar populations to ensure that Spiral galaxies are rejected.
3. `fracDev_r` > 0.95.—The *r* band traces bulge populations and so will select bulges that follow an $r^{1/4}$ profile.
4. `fracDev_i` > 0.95.—The *i* band strengthens the constraint derived from the *r* band profile.

For relatively bright galaxies ($r < 16.8$), this method is very reliable. The number of galaxies accepted that do not appear to be early-types on visual inspection is on the order of ∼15%. Similarly, the number of galaxies that appear to be early-types among those which are rejected due to low values of `fracDev` is ∼10%, which gives us confidence that we are not excluding a significant part of the early-type population. This level of contamination nevertheless requires a careful visual inspection, which is performed after the matching process.

2.2. *Matching to GALEX-MIS*

The initial selection of early-type galaxies in SDSS DR3 yields a total of 89248 galaxies without any constraints on luminosity or redshift. The detections in the *GALEX* MIS survey are then cross-matched to this catalog. All early-type galaxies within each *GALEX* field of view (FOV) are flagged and retained. We then perform a simple proximity search algorithm to find all those *GALEX* detections that are within the 4″ angular resolution limit of *GALEX* of each SDSS early-type. All unique matches are flagged and kept together with all galaxies within *GALEX* fields that are not detected.

2.3. *Visual Inspection of Galaxy Morphology*

The most dangerous contaminant when constructing a sample of supposed early-type galaxies are Sa galaxies. We set the difference between S0 (which we keep) and Sa (which we reject) to be *the presence of distinct spiral arms*. This can be challenging when the galaxies in question are at higher redshift or faint.

In order to quantify how well we can distinguish Sa galaxies based on SDSS images alone, we compare these to the COMBO-17 S11 field, which overlaps with SDSS DR3 and has a number of galaxies at $0.10 \lesssim z \lesssim 0.13$. This image is significantly deeper (24,000 s) and has better seeing (∼0.7″) than SDSS images, so it allows us to identify morphology with much higher accuracy. We selected the brightest galaxies in the S11 field, ranging in *R*-band magnitude from 16.56 to 17.31. From this experiment, we conclude that the reliability of visual inspection is dependent first on redshift and seeing and second on apparent magnitude. In order to set a reliable redshift and magnitude limit, we limit our sample to $z < 0.1$ and $r < 16.8$.

2.4. *The Volume-limited Sample*

In order to create an unbiased sample, we need to take into account a number of factors. At $z < 0.05$, SDSS spectroscopy begins to be incomplete for bright galaxies, so $z = 0.05$ is our lower limit (Stoughton et al. 2002; Strauss et al. 2002).

The *GALEX* MIS limiting magnitude in NUV is 23.0 AB (Morrissey et al. 2005), but many fields have longer exposure and some have been visited multiple times and co-added, giving us no uniform NUV magnitude limit. This is a problem since if we wished to probe the reddest early-types out to NUV − $r \sim 7.5$, we could only probe the most massive galaxies within a small redshift slice. In order to maximize the range in absolute magnitude to a reasonable part of the high end of the luminosity function, we must leave the reddest galaxies incomplete in some fields. We nevertheless retain them as nondetections.

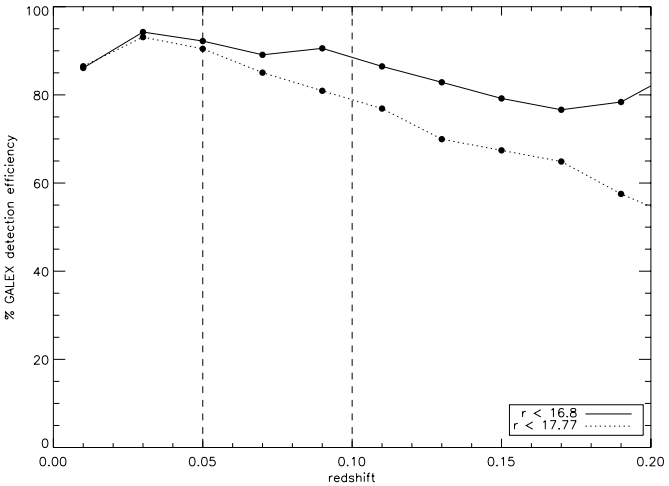

FIG. 1.—Fraction of early-type galaxies in the SDSS -MIS catalog with *GALEX* counterparts as a function of redshift. Within the range $z = [0.05, 0.10]$, the detection efficiency for our sample is stable around ∼90%.

If we choose $r < 16.8$ as an apparent magnitude limit out to which visual inspection can be done reliably, the NUV = 23.0 hard limit guarantees us completeness to NUV − $r = 6.2$, which corresponds roughly to the top of the red sequence introduced by Yi et al. (2005, Fig. 3). However, the fact that many images go up to a magnitude deeper than NUV = 23.0 means we can still probe the red end of the UV color-magnitude relation. Colors redder than NUV − $r \sim 6.5$ cannot be produced by an old stellar population of any age on its own; these galaxies must contain dust to achieve such red colors. Since we are primarily interested in studying those early-type galaxies that show signs of recent star formation, this is a safe limit.

In addition to this, there is a significant fraction of SDSS galaxies in the *GALEX* field of view that are not matched to *any* *GALEX* counterpart (Fig. 1). Even when matching to a sample of spectroscopic galaxies of *all* morphologies in SDSS, roughly 10% do not have *GALEX* detections (Fig. 1). Thus, we must assume that they are either too faint in the UV, too dusty, or a combination of both and so can be assumed to be red on the UV color-magnitude diagram for the purpose of deriving the fractions of UV-bright galaxies. Some of these nondetections might also be due to mechanical problems in astrometry near the edge of the detector. Nevertheless, by making a number of assumptions on these nondetections, we can still derive some information from them.

At $z = 0.1$, $r = 16.8$ is equivalent to an absolute magnitude limit of $M_r = -21.5$, so the limits on our sample are $z = [0.05, 0.10]$ and the color-magnitude relation can be probed out to $M_r = -21.5$. For comparison, $M_* = -20.83$ for all morphologies in an SDSS sample (Blanton et al. 2001).

We then perform a visual inspection of all matched galaxies in our sample and place them into one of three categories:

1. elliptical galaxies (847);
2. lenticular galaxy (112);
3. other (126).

The "other" category includes all galaxies rejected for either non early-type morphology or for the presence of nearby, bright blue stars that might contaminate the UV flux. The apparently low number of lenticular galaxies is due to the fact that we were very stringent about giving out the label "lenticular." If there was any doubt between elliptical and S0, we placed it in the elliptical

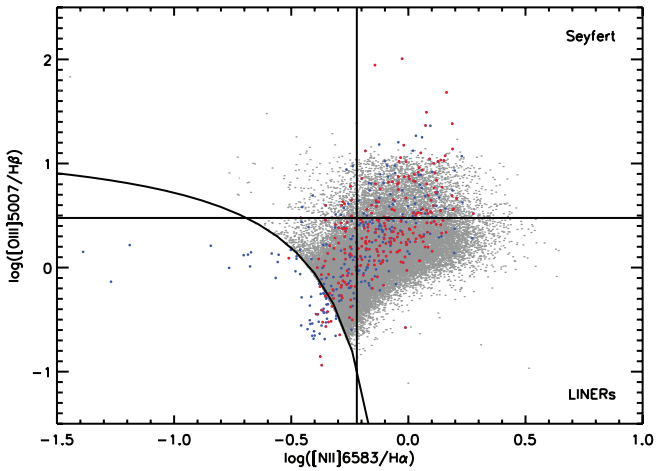

FIG. 2.—BPT diagram for all galaxies with all four emission lines (O III, N II, Hα, Hβ). The red points are classified as early-types by the visual inspection and the blue ones as late-types. The gray points are data from Kauffmann et al. 2003. The diagram is from Kaviraj et al. (2007). The line ratios used are N II/Hα on the x-axis and O III/Hβ on the y-axis. The reason why most objects appear in the AGN regions is that in fact most of our genuine early-type galaxies do not have significant emission lines to be classified here. Those that do tend to be AGNs, rather than star-forming.

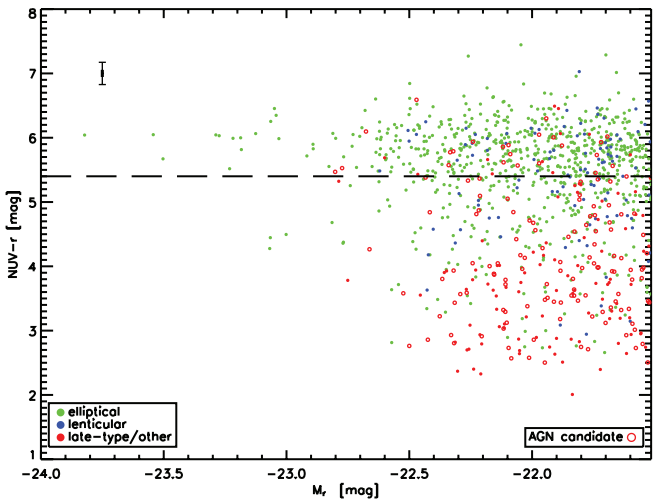

FIG. 3.—Volume-limited UV color-magnitude relation. In green, we show ellipticals and in blue lenticulars galaxies. Red dots denote galaxies that were rejected during the visual inspection as late-types. The red circles show those galaxies that are host to a strong AGN as classified by the BPT diagram. The dashed line indicates the NUV $- r = 5.4$ cutoff for recent star formation. The fraction of UV blue galaxies that are not genuine early-type galaxies is significant: both late-types and AGN candidates are significantly bluer. The error bars in the top left show typical 1 σ errors, although the reddest galaxies may have slightly larger errors as they tend to be very faint in the NUV.

category. In a study of 146 early-type galaxies of the Coma cluster, Jorgensen & Franx (1994) find that the separation of early-type galaxies into elliptical and lenticular is very difficult and that many face-on lenticulars have been misclassified as elliptical galaxies. In § 5.1, we discuss the relationship between recent star formation and axis ratio, where this effect becomes important.

2.5. *Discussion of Random and Systematic Errors*

The random errors in the NUV $- r$ color are dominated by the errors in the NUV. The mean 1 σ error is 0.17 mag, which is much smaller than the overall scatter of the observed colors (Figs. 3 and 6). The *GALEX* photometry are taken from Internal Release 1.1, which is known to underestimate the errors. The errors are recalculated for our analysis following the instruction given in the *GALEX* Web site. Virtually all of our galaxies are unresolved in *GALEX* NUV due to the large size of the NUV point spread function (4″ FHWM). Due to this large difference between the optical and UV resolutions, we do not attempt to use matched apertures. Since we use total fluxes, we do not expect color gradients to affect NUV $- r$ colors.

2.6. *AGN Contamination and Removal*

The other major problem is the presence of AGNs. In the local universe, AGN hosts are preferentially massive elliptical galaxies. A strong AGN can easily produce a UV flux similar to that of a small mass fraction of young stars. In order to minimize the contamination from the galaxies whose UV fluxes are possibly dominated by an AGN nonthermal spectrum rather than a thermal stellar spectrum, we apply two methods.

First, we perform a BPT analysis (Baldwin et al. 1981), wherein galaxies are classified using a number of emission line ratios into either quiescent, star-forming, or AGN. We employ a method similar to the one devised by Kauffmann et al. (2003). The line ratios used are [N II]/Hα and [O III]/Hβ. A full description of our method can be found in Kaviraj et al. (2007).

Classification using such a BPT diagram is only reliable when all four emission lines have sufficient S/N. The S/N cut we employ in this study is S/N > 3 for all four lines. We reject all galaxies consequently classified as Seyfert, LINER or transition objects and only retain those which are quiescent or star-forming. It is interesting to note that most objects classified as star-forming were in fact galaxies rejected by the visual inspection as late-types (see Fig. 2). Most of our early-type galaxies do not appear in Figure 2 because they do not show emission lines with S/N > 3. For a discussion of how the AGNs were identified, see Kauffmann et al. (2003).

This process removed 11% of our volume-limited sample after visual inspection. In order to ensure that we have as few AGNs as possible left in our sample, we checked if any strong radio sources were left. The VLA FIRST survey (Becker et al. 1995) covers about 80% of our galaxies at 1.4 GHz with 5″ resolution. We removed all strong radio sources with a luminosity $L_{1.4\,\mathrm{Ghz}} > 10^{23}$ W Hz^{-1}. This cutoff was chosen as it is often assumed that below this luminosity, AGN activity, and star formation are degenerate, whereas above it, most sources are AGNs. We cross-checked this value to be consistent with the radio luminosities of our BPT-selected AGNs. We only identify 8 further sources, which gives us confidence in the reliability of our BPT diagnostics. In total, this leaves us with a sample of 839 early-type galaxies to analyze. A catalog of these 839 galaxies can be made available on request.

We now construct the UV color-magnitude relation using this sample. In Figure 3, we show the entire sample of *GALEX*-SDSS matches with their classification into early-types, rejected late-types, and AGN candidates.

3. METHOD

In this section we describe our methods for classifying environment and for how we separate recent star formation (RSF) galaxies from "UV-upturn" galaxies.

3.1. *Defining a Parameter for Local Environment*

We wish to define *a quantitative way for measuring environment* that makes as much use of the information we are given as possible. Two-dimensional projected number densities would offer

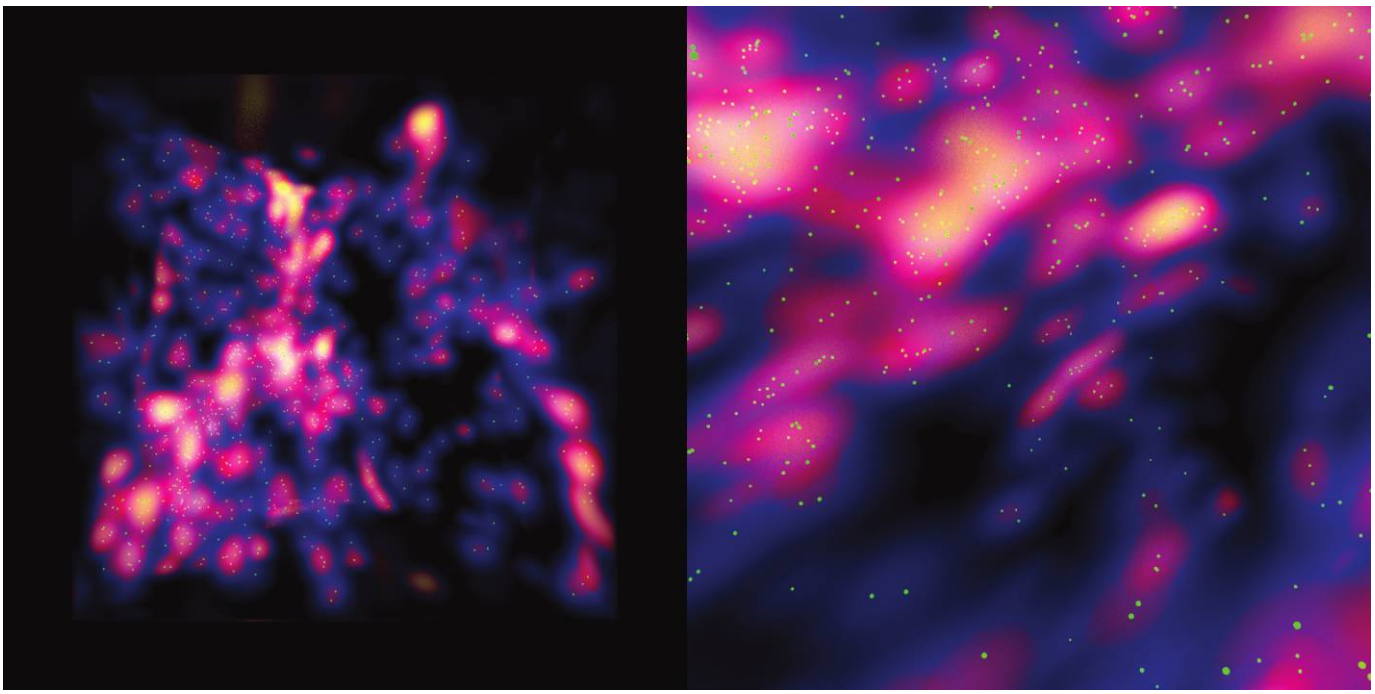

FIG. 4.—Two visualizations of a 3D map of ρ_g. *Left*: a cube of size 100 Mpc from SDSS. We computed ρ_g on a grid with a spacing of 0.5 Mpc. The green spheres represent those galaxies brighter than $M_r < -20.5$ used to compute ρ_g. In terms of the binning scheme outlined in Table 1, transparent corresponds to a value of 0, blue to low density, red to medium density, and yellow to high density. *Right*: a view from inside this cube showing the details of several dense clusters next to a void.

some information, but without redshift information, they can easily be rendered meaningless for anything but the most nearby clusters (e.g., Coma) due to fore- and background contaminants. It is possible to apply statistical methods to correct for this, but since SDSS spectroscopy is available to us for all our galaxies and their surroundings, we can make use of spectroscopic redshifts to determine proximity.

The high-redshift accuracy of SDSS spectroscopy ($\sigma_z = 1.7 \times 10^{-4} \pm 2 \times 10^{-5}$ for our sample, corresponding to $\sim$0.5 Mpc in our redshift range) allows us to compute the number density of neighboring galaxies (Strauss et al. 2002). The SDSS spectroscopic completeness limit of $r = 17.77$ imposes a cutoff in absolute magnitude of $M_r = -20.55$ at our upper redshift limit of $z = 0.1$. This allows us to sample the luminosity function to about M_*, which for an SDSS sample is $M_* = -20.83$ (Blanton et al. 2001).

Any method that relies on number density has to deal with the fact that dense clusters give rise to peculiar velocities that can translate to shifts of up to several hundred km s^{-1}, which can correspond to shifts of up to $\sim$10 Mpc. Hogg et al. (2004), for example, use a cylindrical volume elongated along the z-axis to 16 h^{-1} Mpc to deal with this. Thus, their method corrects as well as is possible for dense environments. However, such a fixed-volume method does not take into account the density-dependence of peculiar velocity.

We therefore attempt to correct for this by employing an adaptive volume: for each galaxy, we initially count all neighbors within a certain radius σ, ignoring the fact that the distance along redshift may be distorted. This number is capped at 10. We use this number n as a guide to adaptively change the extent of our redshift search radius. We define the scale factor c_z as follows:

$$c_z = 1 + 0.2n. \tag{1}$$

The scale factor is used to scale the value of σ along the redshift axis by up to a factor of 3 for the highest density environments to compensate for the "finger-of-God" effect. This is only a zeroth-order approximation, however, and modeling will be needed to devise a more reliable method for scaling to a realistic volume.

We then employ a Gaussian distribution to give more weight to closer neighbors and use c_z to increase the extent of this Gaussian along the z-axis. We define the *adaptive Gaussian environment parameter* ρ_g as the sum over all neighbors within the ellipse defined by

$$\left(\frac{r_a}{3\sigma}\right)^2 + \left(\frac{r_z}{3c_z\sigma}\right)^2 \leq 1, \tag{2}$$

that is, we search out to 3 σ:

$$\rho_g(\sigma) = \frac{1}{\sqrt{2\pi}\sigma} \exp\left[-\frac{1}{2}\left(\frac{r_a^2}{\sigma^2} + \frac{r_z^2}{c_z^2\sigma^2}\right)\right], \tag{3}$$

where r_a is the angular distance in Mpc to each surrounding galaxy, r_z is the distance along the line of sight in Mpc to each surrounding galaxy, and σ is an arbitrary dispersion parameter. This weighting scheme is biased toward nearby galaxies and so is a more realistic measure than a raw number density or overdensity. When measuring this parameter for a particular galaxy, the galaxy itself is *not* counted toward the total. For this project, we adopt a fiducial value of σ of 2.0 Mpc. The choice of $\sigma =$ 2 Mpc is somewhat arbitrary. We chose it so that the scale length of our measure was focused approximately on the scale of large groups and small clusters. Perturbing σ does not change our results within 1 σ.

But what does this parameter actually measure? It is blind as to whether the structure around it is gravitationally bound or in equilibrium, so it is not a way of separating clusters from the field. Rather, it is a measure of the number and proximity of galaxies around a point in space, a more sophisticated number density. Despite that, it is useful to have physical sense on the values of

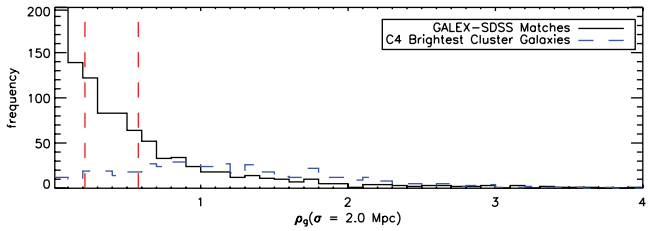

FIG. 5.—Distribution of ρ_g for the volume-limited sample (*black*) and the brightest cluster galaxies in the C4 cluster catalog for those clusters in the redshift range $z = [0.05, 0.10]$ (*blue*). The red lines indicate the cutoffs for the three environment bins (see Table 1 Of the C4 BCGs, 5.1% lie in the low bin, 14.4% lie in the medium bin, and 80.5% are in the high bin. Those C4 clusters in the low bin are generally very small clusters or groups when viewed in SDSS.

ρ_g. First of all, the spatial distribution of our galaxies is mapped in Figure 4.[10] The brighter regions are denser. For comparison, we compute ρ_g for the bright cluster galaxies in the C4 Catalog (Miller et al. 2005) within our redshift range. Indeed, most of them have high values of ρ_g (Fig. 5). Typically, the central galaxy of a typical cluster with 10 L_* galaxies randomly distributed within a $r \sim 3$ Mpc sphere would have $\rho_g \sim 1$. A galaxy at the edge of the same cluster, however, would have $\rho_g \sim 0.5$. All galaxies in a group with three L_* galaxies within a $r \sim 1$ Mpc sphere would have similar values of ρ_g to the cluster outskirts. Typical field galaxies would have $\rho_g \lesssim 0.2$. We divide our final sample into three numerically equal environment bins, which we arbitrarily label "low," "medium," and "high" density (see Table 1). The (1) low, (2) medium, and (3) high density roughly correspond to (1) fields, (2) groups and cluster outskirts, and (3) cluster centers, respectively.

We also tested whether a mass weight could improve our measure. We tested a weight of the form

$$\rho_g(\sigma) = \frac{f(\mathrm{mass})}{\sqrt{2\pi}\sigma} \exp\left[-\frac{1}{2}\left(\frac{r_a^2}{\sigma^2} + \frac{r_z^2}{c_z^2\sigma^2}\right)\right], \qquad (4)$$

where we chose f to be a linear function of absolute r-band magnitude such that a galaxy at the lower limit of $M_r = -20.55$ counted as 1 and the most massive neighbors of $M_r \sim -23$ counted 3 times as much. This made no difference within error to our result, so we do not use such a mass weight to avoid introducing unnecessary complication, so we adopt $f(\mathrm{mass}) = 1$.

3.2. *Recent Star Formation and the UV-Upturn Phenomenon*

Many early-type galaxies exhibit the UV-upturn phenomenon (Code & Welch 1979; Burstein et al. 1988) characterized by unusually strong UV flux rising with decreasing wavelength in the range (1000–2500 Å). The UV-upturn phenomenon is thought to be due to the presence of low-mass, core helium-burning horizontal branch (HB) and evolved HB stars (Yi et al. 1997). We therefore face the problem that the moderate UV flux that we see in many of our early-type galaxies may in fact be due to such an old stellar population, or, even more difficult to resolve, due to both old and young stars.

There is, however, a limit to how much NUV flux an early-type galaxy can produce via UV-upturn. This limit can be explored using both theoretical and observational methods. Ideally, we wish to combine both to derive a conservative limit beyond which we can be certain to probe recent star formation only. However, the UV upturn theory is still debated, and thus observational evidence should take precedence.

The *IUE* satellite conducted a survey of UV spectra of nearby elliptical galaxies (Burstein et al. 1988). Among the strongest known nearby UV-upturn galaxies is NGC 4552, which has an NUV $- r$ color of 5.4 mag. We therefore choose NUV $- r = 5.4$ as a conservative lower boundary in color. At NUV $- r < 5.4$, all galaxies are considered to have experienced a recent episode of star formation, although part of their UV flux may come from a

[10] Created using POV-ray (http://www.povray.org).

TABLE 1
ENVIRONMENT BINS

Bin	$\rho_g(\sigma = 2.0$ Mpc)	Label
$0 - \frac{1}{3}$	$0.00 < \rho_g \leq 0.21$	Low density
$\frac{1}{3} - \frac{2}{3}$	$0.21 < \rho_g \leq 0.58$	Medium density
$\frac{2}{3} - 1$	$0.58 < \rho_g \leq 4.68$	High density

NOTES.—These bins are derived by splitting our sample of 839 galaxies into three equal-number bins. The values of ρ_g represent the boundaries between them.

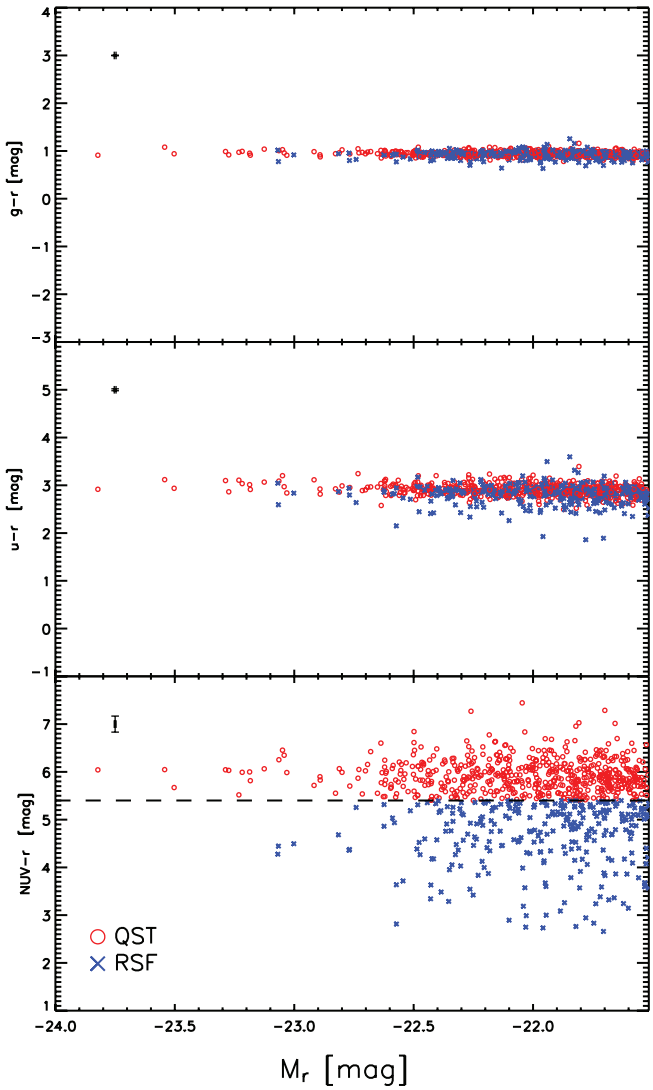

FIG. 6.—Color-magnitude relations of our final-selection early-type galaxies. In the lowest panel, we show the NUV $- r$ CMR and color-code those galaxies classified as RSF (See § 3.2) blue. We compare these to the optical $u - r$ and $g - r$ CMRs. In optical colors, RSF and QST galaxies are completely degenerate with each other. Even u band shows only a slight shift toward the blue of RSF galaxies compared to quiescent ones and a slightly larger scatter. We do not show either late-types or AGN candidates. In each panel, we show typical 1 σ errors.

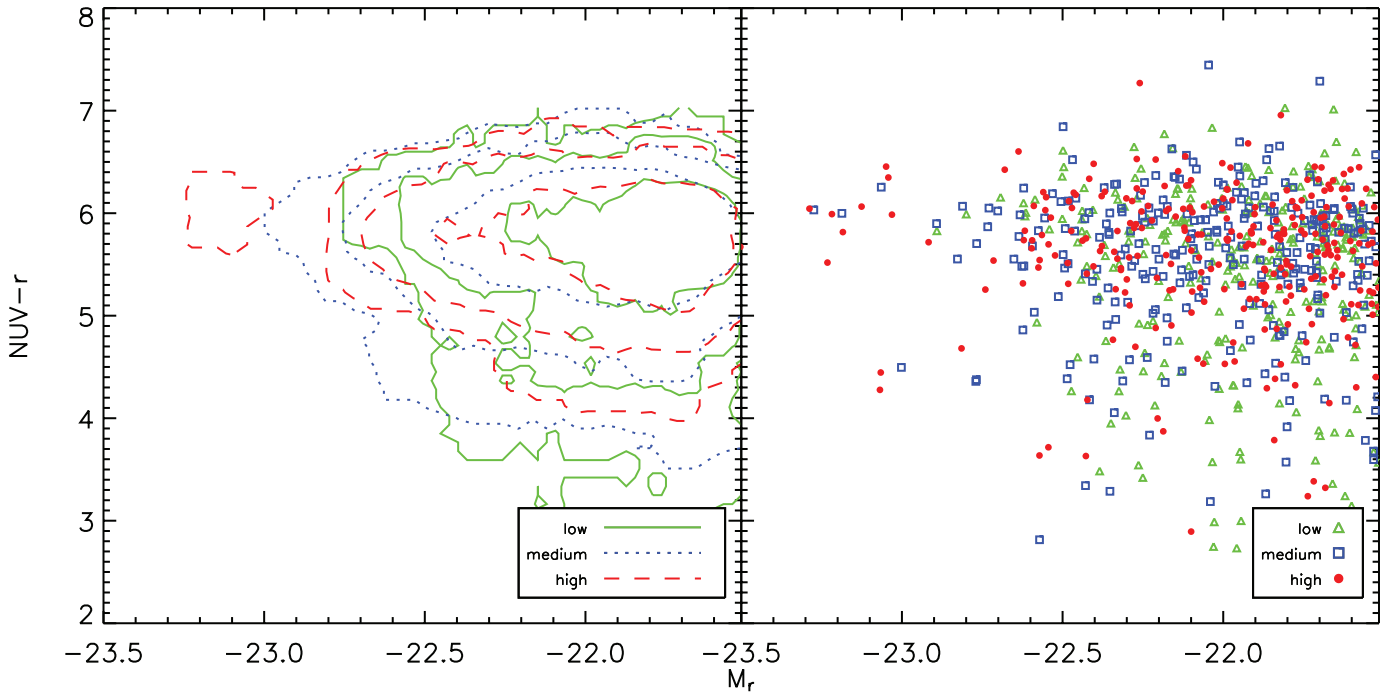

FIG. 7.—*Left*: Contour plot of the UV color-magnitude relation split into three equal-number environment bins (See Table 1). The contour curves enclose 93%, 80%, and 50% of galaxies. *Right*: the actual data points. *Green triangles*, low density; *blue squares*, medium density; *red dots*, high density. There are two differences with environment: Higher mass galaxies prefer to reside in high-density environments and low-mass galaxies are bluer.

UV-upturn. Above this limit, a galaxy might either (or both) be forming stars or (and) exhibiting UV-upturn—we cannot distinguish the two using *GALEX* NUV alone. Considering that the *IUE* SEDs were obtained from the UV-bright central regions of galaxies, our NUV $- r = 5.4$ cut is conservative and puts some fraction of star-forming galaxies into the quiescent galaxy bins.

3.3. *Comparison between the Optical and UV-CMR*

In Figure 6, we plot the optical $u - r$ and $g - r$ color-magnitude relations on the same scale as the NUV $- r$. We label galaxies not classified as AGNs by the BPT diagram above NUV $- r = 5.4$ as quiescent (QST) and those bluer as recent star formation (RSF). We do not include a slope in this cutoff, although one might suggest a slope based on the red-sequence slope, for example as found by Yi et al. (2005, Fig. 3), because any slope over our magnitude range would likely be very small and complex (albeit not impossible) to explain theoretically. We can see that the $g - r$ is completely insensitive. It cannot be used to detect recent star formation in early-type galaxies. Even $u - r$ color does not break this degeneracy. While the scatter of the UV-bright RSF galaxies is slightly greater, the bulk of them are indistinguishable from quiescent ones. In order to properly study recent star formation in early-type galaxies the UV information is essential.

In total, 30% $\pm$ 3% of our 839 early-type galaxies with $M_r < -21.5$ are classified as RSF using this scheme. This RSF galaxy fraction is probably a lower limit, first because of our conservative UV-upturn criterion and because we do not correct our UV data for internal extinction.

4. THE EFFECT OF ENVIRONMENT ON EARLY-TYPE GALAXIES

In this section, we investigate two related questions: does the UV color-magnitude relation depend on environment? And does the *fraction* of early-type galaxies showing signs of recent star formation depend on environment?

4.1. *The Color-Magnitude Relation and Environment*

It is well known that more massive early-type galaxies reside in denser environments (Dressler 1980; Postman & Geller 1984) even though the slope and zero point of their color-magnitude relations do not appear to depend on environment. Hogg et al. (2004) find that (1) the color-magnitude relation for their sample of 55,158 early-type galaxies in SDSS does not depend on environment and that (2) the most luminous galaxies reside preferentially in the most high-density environments. Finding (2) is not surprising as the most massive ellipticals are known to reside at the centers of clusters (Beers & Geller 1983).

In their analysis, Bernardi et al. (2003b) also find little dependence of the color-sigma relation on environment. Furthermore, Bernardi et al. (2005) suggest that the color-magnitude relation is entirely a consequence of the fact that both the luminosities and colors are correlated with sigma, a proxy to mass; that the color-sigma relation is in fact the more fundamental relation.

In Figure 7, we show the UV color-magnitude relation for the three equal-number environment bins defined in Table 1. From this, we can see that there are two obvious differences between the low-, medium-, and high-density color-magnitude relations. As expected, the higher density CMR extends to more massive galaxies. However, the low-density CMR extends to bluer colors than the high-density one. This is observational evidence for a change in the range of color of the UV-CMR with environment. We test the statistical significance of both of these environmental differences.

4.2. *The Dependence of* NUV $- r$ *Color on Environment*

The first quantity we consider is NUV $- r$ color. In Figure 8, we show how NUV $- r$ color varies with ρ_g. The range in NUV $- r$ remains more or less constant over the entire range of ρ_g, but the distribution itself varies with ρ_g. We can make this variation more apparent by plotting the cumulative color distribution of the three environment bins in Figure 8. In this plot, we not only show the

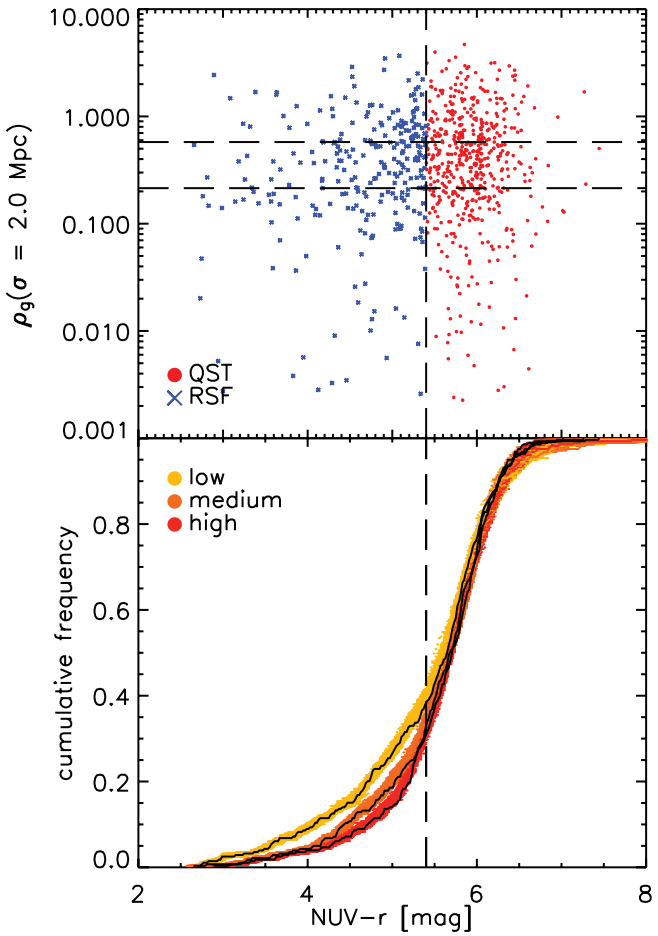

FIG. 8.—*Top*: Distribution of NUV − *r* color with environment. The vertical line indicates the RSF-QST cutoff, and the horizontal lines the environment bins (see Table 1). *Bottom*: Cumulative distribution of NUV − *r* color for each environment bin. Around each cumulative curve (*in black*), we plot 100 Monte Carlo resimulations of the NUV − *r* color distribution taking the errors in the colors into account. The enhancement at blue colors for low-density galaxies remains pronounced.

cumulative distribution itself, but also a Monte Carlo resimulation of the color distribution. In order to assess to what extent the difference between the environment bins is, we regenerate the distribution by randomly changing the color by the error and recomputing the distribution.

The "medium" and "high" density curves are statistically indistinguishable. On the other hand, the low-density bin (Fig. 8, *yellow line*) diverges from the other two at blue colors. We test the significance of this difference using both Kolmogorov-Smirnov (KS) and Kuiper test. The test significances are the probability that one of the distributions is drawn from a different parent distribution. The results are shown in Tables 2 and 3.

TABLE 2

K-S TEST OF NUV − *r* COLOR DEPENDENCE ON ENVIRONMENT

Bin	Low	Medium	High
Low	...	89.220%	99.239%
Medium	89.220%	...	25.130%
High	99.239%	25.130%	...

NOTE.—Table of Kolmogorov-Smirnov test significance comparing the distribution of NUV − *r* color in the three environment bins.

TABLE 3

KUIPER TEST OF NUV − *r* COLOR DEPENDENCE ON ENVIRONMENT

Bin	Low	Medium	High
Low	...	83.428%	99.657%
Medium	83.428%	...	55.753%
High	99.657%	55.753%	...

NOTE.—Table of Kuiper test significance comparing the distribution of NUV − *r* color in the three environment bins.

4.3. *The Dependence of Mass on Environment*

Figure 9 shows how M_r varies with ρ_g. If we then plot the cumulative M_r distribution for the three environment bins (Fig. 9), we see a clear dependence of absolute magnitude on environment. Even in our volume-limited sample with a narrow baseline in luminosity there is a clear trend for brighter galaxies to be in higher density environments. In Table 4, we give the KS-test significance for the differences between the M_r distributions in each bin.

5. THE DEPENDENCE OF RECENT STAR FORMATION ACTIVITY ON ENVIRONMENT

The fact that the distribution of NUV − *r* color of massive early-type galaxies changes between low- and high-density environments may suggest that the recent star formation history of those galaxies is different. In order to quantify this, we use the criterion for recent star formation outlined in § 3.2. It is not possible

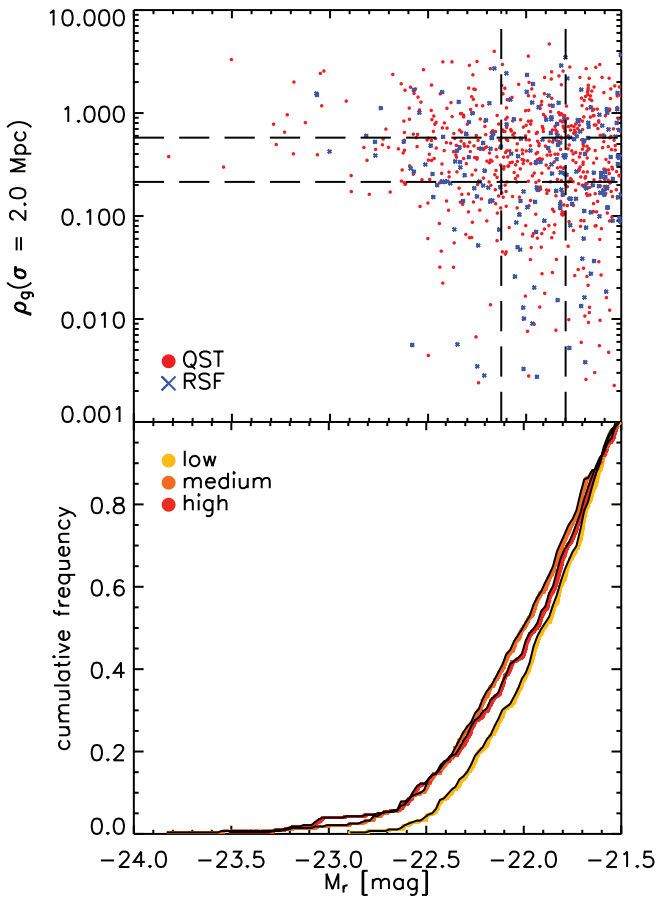

FIG. 9.—*Top*: Distribution of M_r with environment. The horizontal lines divide the environment bins (see Table 1). *Bottom*: Cumulative distribution of M_r for each environment bin. Like for NUV − *r* color, we display an MC resimulation of the M_r distribution. The errors in M_r are much smaller.

TABLE 4
K-S Test of r-Band Absolute Magnitude Dependence on Environment

Bin	Low	Medium	High
Low	...	99.139%	90.816%
Medium	99.139%	...	50.728%
High	90.816%	50.728%	...

Note.—Table of Kolmogorov-Smirnov test significance comparing the distribution of M_r in the three environment bins.

to directly convert NUV flux into an actual star formation rate, chiefly due to our inability to quantify dust extinction, to which the near-UV is extremely sensitive. We therefore merely classify our galaxies as RSF and QST and calculate the RSF galaxy fractions for subsamples in different environments in an attempt to find general trends.

We calculate the recent star-forming fraction of early-types by dividing the number of galaxies bluer than NUV $- r = 5.4$ (RSF) by the total number of galaxies in this bin—that is, both those bluer and redder than NUV $- r = 5.4$ as well as those not detected by *GALEX* but classified as early-type galaxies during the visual inspection. We include these nondetections as QSTs on the assumption that they are red galaxies further reddened by dust beyond the MIS detection limit. It is an intriguing possibility that at least some of these galaxies are dusty because they are actually forming stars, but we cannot make this distinction using *GALEX*.

In total, 30% $\pm$ 3% of our 839 early-type galaxies with $M_r < -21.5$ are classified as RSF. The ellipticals, the bulk of our sample, have an RSF fraction of 29% $\pm$ 3%, while the lenticulars have an RSF fraction of 39% $\pm$ 5%. The division into ellipticals and lenticulars is based on visual inspection. We mentioned in § 2.4 that our visual classification was generous to ellipticals. Hence, if half of our ellipticals were in truth lenticulars, and if 39% were the true RSF galaxy fraction for lenticulars, the RSF fraction for true ellipticals would be as low as 20%.

5.1. *RSF and Axis Ratio*

The RSF galaxy fraction of those galaxies identified as lenticulars in the visual inspection is higher than that of the ellipticals.

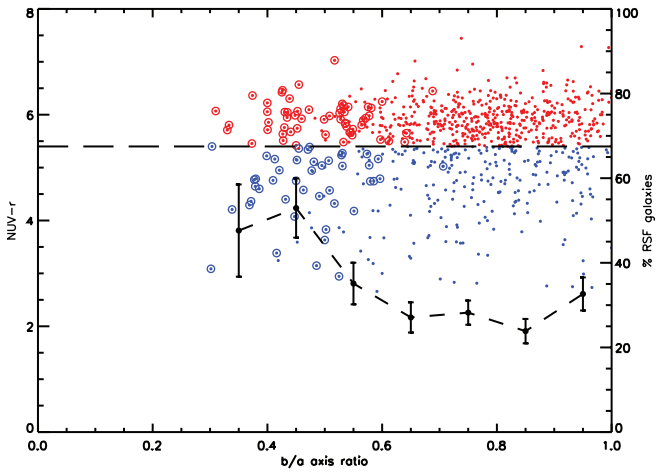

Fig. 10.—Distribution of NUV $- r$ color with r-band b/a axis ratio. The number of RSF galaxies remains roughly constant with axis ratio. Even some of the roundest ellipticals are classified as RSF. In contrast, QST galaxies cluster around high axis ratios and so the fraction of RSF galaxies increases at very low axis ratios. Those galaxies identified as lenticulars are surrounded by a circle; they cluster at low values of b/a, as expected. None of our visually identified lenticulars lie at high values of b/a, confirming the bias against identifying face-on lenticulars as lenticulars.

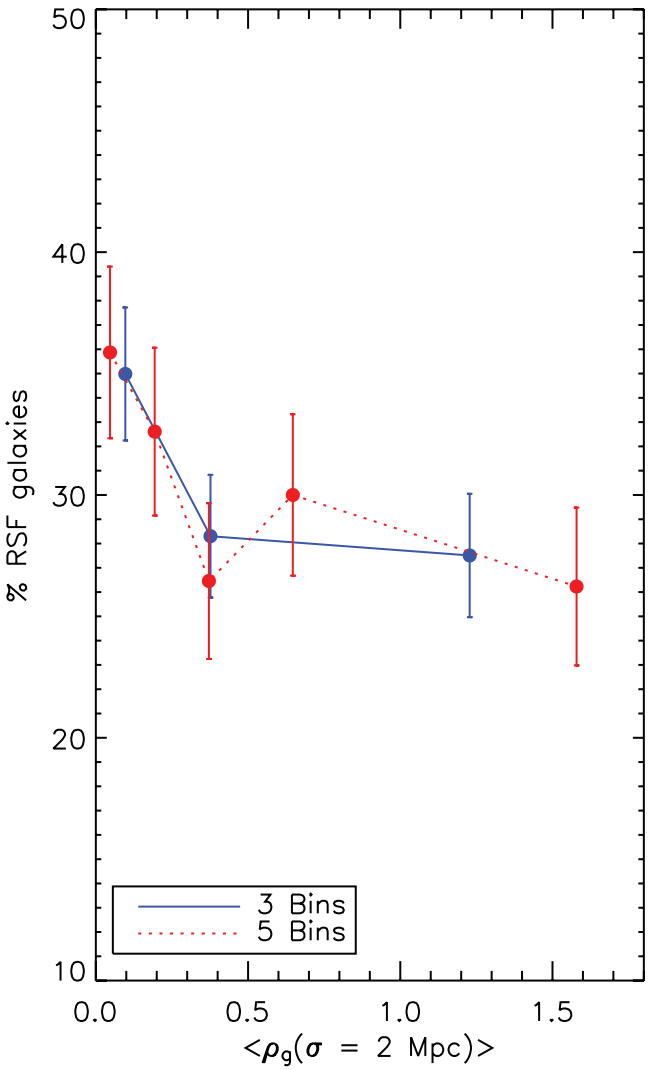

Fig. 11.—Fraction of early-type galaxies that are classified as actively star-forming as a function of environment, binned into 3 and 5 equal-number bins. The points are plotted at the *mean* value of ρ_g in that particular bin.

While there is no natural way to distinguish ellipticals and lenticulars (Jorgensen & Franx 1994), we can look at the change in UV properties with axis ratio. This still suffers from the fact that orientation can obscure true axis ratio. In Figure 10, we show the distribution of NUV $- r$ color with r-band axis ratio together with the RSF percentage as a function of b/a. Even among the roundest elliptical galaxies such as E0/1, there still is a significant fraction of star-forming galaxies. The RSF percentage appears to have a weak dependence on b/a rising up to ~50% for the most flattened galaxies (which corresponds to the 39% we find for the visually identified lenticulars), but the trend is statistically insignificant. All this should be viewed in light of the bias against visually identifying face-on lenticular galaxies (Jorgensen & Franx 1994); it is likely that a fraction of the round early-types are such misclassified objects and that the RSF fraction for genuine, round ellipticals is lower.

5.2. *The Dependence of the RSF Galaxy Fraction on Environment*

We now divide our sample into the three equal-number environment bins (see Table 1) to see whether the RSF fraction depends on environment. As expected from the results in § 4.2, the

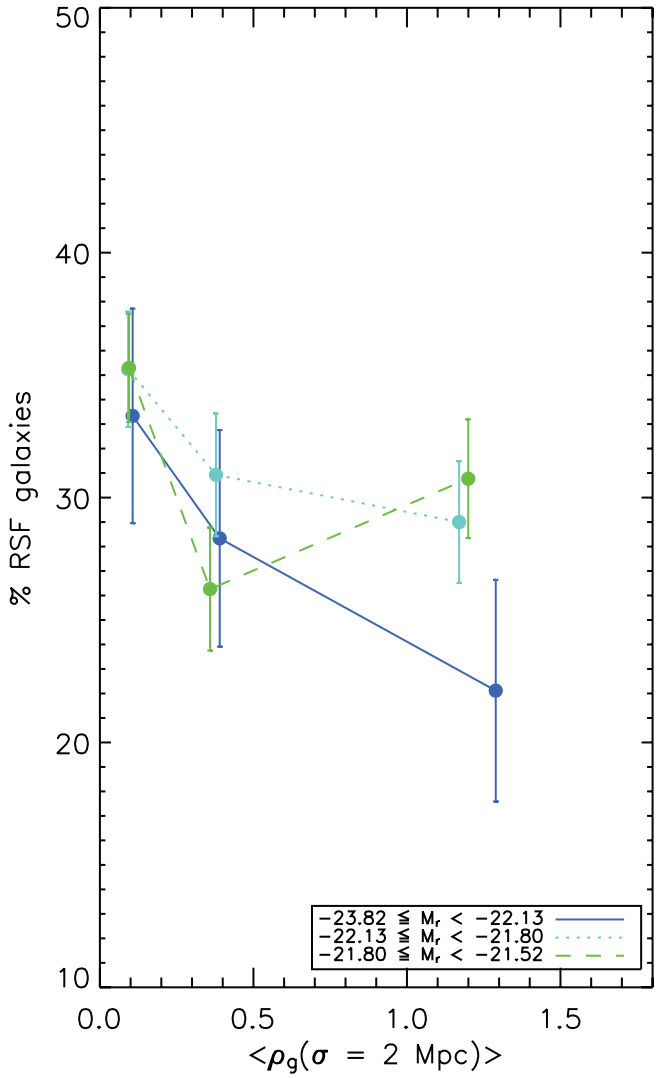

FIG. 12.—In order to break the degeneracy between mass and environment, we bin our sample into three equal-number M_r bins. The enhancement of the RSF-fraction at low density is still present in all three bins and so is at least not entirely due to a mass effect. The points are plotted at the *mean* value of ρ_g in that particular bin.

low-density environment bin shows a pronounced enhancement of the fraction of galaxies showing signs of recent star formation (see Fig. 11). The medium- and high-density bins are consistent with having the same fraction.

In order to constrain this enhancement further, we then divide our sample into five equal-number bins to see at what values of ρ_g this increase lies and in particular whether there is any change at very low or high values. The red five-bin curve in Figure 11 shows that there is no change at high density and that the enhancement of the fraction of RSF galaxies begins at values of $\rho_g \sim 0.4$. This corresponds roughly to one M_* galaxy per cubic megaparsec, a loose definition of the "field." Thus, the enhancement of star formation in our sample is primarily due to the galaxies in the field. Our environment parameter on the other hand only probes neighbors down to $M_r \sim -20.5$, so these galaxies may well merely lack large neighbors—that they may simply be the dominant galaxy in a small group.

Large surveys of galaxy star formation rates show a strong dependence on environment. Studies in both 2dF (Lewis et al. 2002) and SDSS. (Gómez et al. 2003) find that above a certain "break" local density, star formation rapidly declines. This "break" or "characteristic" local Galactic density is given as $\sim 1\ h^2\ \mathrm{Mpc}^2$, so the enhancement we see is similar. However, they also find a continuing decrease in star formation rate with increasing Galactic density, which we do *not* see. A direct comparison to our result is not possible however, since we cannot trace actual star formation rates, but rather only the fraction of galaxies showing signs of *recent* star formation.

5.3. *Breaking the Mass-Environment Degeneracy*

In § 4.3, we have shown the well-known fact that more massive galaxies prefer higher density environments. It is also well-known that smaller galaxies tend to have higher star formation rates and are bluer, i.e., that the color-magnitude relation has a slope. This raises the possibility that the dependence of the RSF fraction for our entire volume-limited sample is nothing but an effect of mass. In order to test whether this is the case, we have to break the mass-environment degeneracy.

Similarly to the environment bins, we divide our sample into three equal-number absolute magnitude bins. Together with the three environment bins, this gives us three curves of RSF percentage as a function of environment like Figure 12. These nine subsamples are indicated by the dashed lines on Figure 9. The resulting curves are shown in Figure 12. From this, it is apparent that the effect of environment that we are seeing is not due to a stellar mass effect, as all three curves follow almost the same trend of a high RSF fraction at low density and a low RSF fraction at high density. Intriguingly, the high-mass bin ($-23.82 < M_r \leq -22.13$) departs from the others at high density, although this remains just above a 1 σ result. It should also be noted that the strongest density dependence is found among the brightest galaxies.

6. SUMMARY

We have used the UV color-magnitude relation of low-redshift, massive early-type galaxies to study their recent star formation history. Our sample is volume-limited, ranging in redshift from $z = 0.05$ to 0.1 and is limited in absolute magnitude to $M_r < -21.5$. Our sample is highly unlikely to be contaminated by any significant number of late-type galaxies, as all our galaxies have been visually inspected.

In order to classify galaxies by their environment, we have devised a method for measuring environment that takes the proximity, and not just the number density of neighboring galaxies, into account (see § 3.1). This method can easily be modified to different samples within SDSS and can take into account a larger part of the luminosity function if restricted to lower redshift limits than $z = 0.1$. Our measure works very well for the brightest cluster galaxies in the C4 cluster catalog and in addition also performs for field galaxies.

In our sample of 839 early-type galaxies with $M_r < -21.5$, the recent star formation (RSF) galaxy fraction is $30\% \pm 2\%$. Our ellipticals, the bulk of our sample, have an RSF fraction of $29\% \pm 3\%$, while the lenticulars show $39\% \pm 5\%$. This implies that *residual star formation is common among the present day early-type galaxy population*. Our estimates are very likely lower limits on the true fractions, as our criteria for RSF are conservative in the consideration of internal extinction and the UV contribution from the old populations.

The UV color-magnitude relation differs from the optical color-magnitude relation (Bower et al. 1992; Hogg et al. 2004) in that it does vary more clearly with environment. The recent star formation history of early-type galaxies also varies with environment. It

is well-known that more massive galaxies reside in higher-density environments (Fig. 9), but we show for the first time that UV-bright early-type galaxies preferentially reside in low-density environments. The RSF fraction is a function of environment and drops by 25% from field to group but then puzzlingly remains relatively constant at higher densities, even when split into luminosity bins (Fig. 12). Interestingly, the most massive galaxies ($-23.82 < M_r \leq -22.13$) show the strongest dependence on environment and alone exhibit a further drop in RSF fraction from medium to high density.

One possible way to understand the drop in the RSF fraction between low and medium density is in the context of ram pressure stripping. Galaxies moving fast in the deep gravitational potential of a galaxy cluster are bound to lose most of their gas during their orbital motion (Gunn & Gott 1972). The density dependence of gas content in galaxies has long been established empirically as well (Giovanelli et al. 1981). Our RSF fraction-density relation is in the right direction. The gas goes into the ICM and so could potentially explain the star formation we do see in high-density environments.

Another noteworthy observation is the fact that those early-type galaxies that have been identified as AGNs—by emission lines and/or radio—are significantly bluer than those that have not (see Fig. 3). We have removed these AGNs from our sample since we cannot disentangle the UV flux from the AGNs from that of a possible young stellar population. However, the blueness of the AGN colors is intriguing—are we really just seeing the AGN itself, or is this from the star formation triggered by the jets and outflows from the AGNs (Silk & Rees 1998)? In the latter case, the RSF fraction would increase further from our estimates, and the AGN regulations might present a possible physical mechanism responsible for the star formation that we observe. In fact, Heckman et al. (1995) using *IUE* observations of nearby type 1 and 2 Seyferts, suggest that at most 20% of the UV continuum emission seen in them can originate from the nucleus itself. This means that the vast majority of our AGN candidates (removed) would qualify as RSF galaxies.

It is important to note that we only deal with *fractions* of star-forming galaxies and not actual star formation rates. Thus, our RSF fractions simply give us an indication of how likely an early-type galaxy with certain properties and in a certain environment is to have experienced recent star formation. Neither environment, luminosity, nor axis ratio seems to be the primary physical quantity that regulates recent star formation in early-type galaxies. The relative insensitivity to environment in any environment denser than the field is also surprising and warrants further study. The observational trends presented here give us new constraints for theoretical models of galaxy evolution.

Special thanks are given to M. Bernardi, who kindly supplied her early-type galaxy catalog, which provided us with a great insight on our catalog generation. We warmly thank C. Wolf for making the *COMBO-17* S11 field image available to us. We would also like to thank E. Gawiser, L. Miller, S. Rawlings, J. Silk, R. Davies, I. Jorgensen, M. Sarzi, J. Magorrian, S. Salim, M. Urry, and K. Kotera for helpful comments and discussions.

GALEX (*Galaxy Evolution Explorer*) is a NASA Small Explorer, launched in 2003 April. We gratefully acknowledge NASA's support for construction, operation, and science analysis for the *GALEX* mission, developed in cooperation with the Centre National d'Etudes Spatiales of France and the Korean Ministry of Science and Technology. This work was supported by grant R01-2006-000-10716-0 from the Basic Research Program of the KOSEF and Yonsei University Research Fund to the corresponding author (S. K. Yi).

REFERENCES

Abazajian, K., Adelman-McCarthy, J. K., Agüeros, M. A., Allam, S. S., Anderson, K. S. J., Anderson, S. F., Annis, J., & Bahcall, N. A. 2005, AJ, 129, 1755
Baldwin, J. A., Phillips, M. M., & Terlevich, R. 1981, PASP, 93, 5
Barnes, J. E. 1988, ApJ, 331, 699
Baum, W. A. 1959, PASP, 71, 106
Becker, R. H., White, R. L., & Helfand, D. J. 1995, ApJ, 450, 559
Beers, T. C., & Geller, M. J. 1983, ApJ, 274, 491
Bernardi, M., Sheth, R. K., Nichol, R. C., Schneider, D. P., & Brinkmann, J. 2005, AJ, 129, 61
Bernardi, M., et al. 2003a, AJ, 125, 1817 (B03)
———. 2003b, AJ, 125, 1882
Blakeslee, J. P., et al. 2003, ApJ, 596, L143
Blanton, M. R., et al. 2001, AJ, 121, 2358
Bower, R. G., Lucey, J. R., & Ellis, R. S. 1992, MNRAS, 254, 589
Bruzual, A., G., & Charlot, S. 1993, ApJ, 405, 538
Burstein, D., Bertola, F., Buson, L. M., Faber, S. M., & Lauer, T. R. 1988, ApJ, 328, 440
Butcher, H., & Oemler, A. 1984, ApJ, 285, 426
Carollo, C. M., & Danziger, I. J. 1994a, MNRAS, 270, 743
———. 1994b, MNRAS, 270, 523
Carollo, C. M., Danziger, I. J., & Buson, L. 1993, MNRAS, 265, 553
Code, A. D., & Welch, G. A. 1979, ApJ, 228, 95
Couch, W. J., Barger, A. J., Smail, I., Ellis, R. S., & Sharples, R. M. 1998, ApJ, 497, 188
de Vaucouleurs, G. 1961, ApJS, 5, 233
Dressler, A. 1980, ApJ, 236, 351
Dressler, A., et al. 1997, ApJ, 490, 577
Eggen, O. J., Lynden-Bell, D., & Sandage, A. R. 1962, ApJ, 136, 748
Ellis, R. S., Smail, I., Dressler, A., Couch, W. J., Oemler, A. J., Butcher, H., & Sharples, R. M. 1997, ApJ, 483, 582
Ferreras, I., Lisker, T., Carollo, C. M., Lilly, S. J., & Mobasher, B. 2005, ApJ, 635, 243
Fukugita, M., Nakamura, O., Turner, E. L., Helmboldt, J., & Nichol, R. C. 2004, ApJ, 601, L127
Gómez, P. L., et al. 2003, ApJ, 584, 210
Giovanelli, R., Haynes, M. P., & Chincarini, G. L. 1981, ApJ, 247, 383
Gladders, M. D., Lopez-Cruz, O., Yee, H. K. C., & Kodama, T. 1998, ApJ, 501, 571
Gunn, J. E., & Gott, J. R. I. 1972, ApJ, 176, 1
Heckman, T., Krolik, J., Meurer, G., Calzetti, D., Kinney, A., Koratkar, A., Leitherer, C., Robert, C., & Wilson, A. 1995, ApJ, 452, 549
Hernquist, L. 1992, ApJ, 400, 460
Hogg, D. W., et al. 2004, ApJ, 601, L29
Jorgensen, I., & Franx, M. 1994, ApJ, 433, 553
Kauffmann, G., Charlot, S., & White, S. D. M. 1996, MNRAS, 283, L117
Kauffmann, G., et al. 2003, MNRAS, 346, 1055
Kaviraj, S., Devriendt, J. E. G., Ferreras, I., & Yi, S. K. 2005, MNRAS, 360, 60
Kaviraj, S., et al. 2007, ApJS, 173, 619
Khochfar, S., & Burkert, A. 2001, ApJ, 561, 517
Kodama, T., & Arimoto, N. 1997, A&A, 320, 41
Larson, R. B. 1974, MNRAS, 169, 229
———. 1975, MNRAS, 173, 671
Lewis, I., et al. 2002, MNRAS, 334, 673
Martin, D. C., et al. 2005, ApJ, 619, L1
McClure, R. D., & van den Bergh, S. 1968, AJ, 73, 1008
Miller, C. J., et al. 2005, AJ, 130, 968
Morrissey, P., et al. 2005, ApJ, 619, L7
Naab, T., & Burkert, A. 2003, ApJ, 597, 893
Negroponte, J., & White, S. D. M. 1983, MNRAS, 205, 1009
Postman, M., & Geller, M. J. 1984, ApJ, 281, 95
Rich, R. M., et al. 2005, ApJ, 619, L107
Silk, J., & Rees, M. J. 1998, A&A, 331, L1
Spergel, D. N., et al. 2003, ApJS, 148, 175
Stanford, S. A., Eisenhardt, P. R., & Dickinson, M. 1998, ApJ, 492, 461
Stoughton, C., Lupton, R. H., Bernardi, M., Blanton, M. R., Burles, S., Castander, F. J., Connolly, A. J., & Eisenstein, D. J. 2002, AJ, 123, 485
Strauss, M. A., et al. 2002, AJ, 124, 1810
Thomas, D., Greggio, L., & Bender, R. 1999, MNRAS, 302, 537
Trager, S. C., Faber, S. M., Worthey, G., & González, J. J. 2000, AJ, 120, 165

van Dokkum, P. G., Franx, M., Fabricant, D., Illingworth, G. D., & Kelson, D. D. 2000, ApJ, 541, 95
van Dokkum, P. G., Franx, M., Fabricant, D., Kelson, D. D., & Illingworth, G. D. 1999, ApJ, 520, L95
White, S. D. M., & Rees, M. J. 1978, MNRAS, 183, 341
Worthey, G., Faber, S. M., & Gonzalez, J. J. 1992, ApJ, 398, 69
Yi, S., Demarque, P., & Oemler, A. J. 1997, ApJ, 486, 201
Yi, S. K., et al. 2005, ApJ, 619, L111
York, D. G., Adelman, J., Anderson, J. E., Anderson, S. F., Annis, J., Bahcall, N. A., Bakken, J. A., & Barkhouser, R. 2000, AJ, 120, 1579